Inorganic Chemistry

Communication

pubs.acs.org/IC

Doubly Interpenetrated Chiral (10,3)-a Network with Charge-Transfer-Type Guest Inclusion

Lei Han,*[,†] Lan Qin,[†] Lan-Ping Xu,[†] and Wen-Na Zhao[‡]

[†]State Key Laboratory Base of Novel Functional Materials and Preparation Science, Faculty of Materials Science & Chemical Engineering, Ningbo University, Ningbo, Zhejiang 315211, China

[‡]Key Laboratory for Molecular Design and Nutrition Engineering of Ningbo, Ningbo Institute of Technology, Zhejiang University, Ningbo, Zhejiang 315100, China

Supporting Information

ABSTRACT: A doubly interpenetrated metal−organic framework, $[Zn_3(TATB)_2(H_2O)_2]_n$ (**2**), with chiral (10,3)-a topology, has been synthesized from an achiral, trigonal-planar ligand, 4,4′,4″-*s*-triazine-2,4,6-triyltribenzoate (TATB). The large chiral channels in **2** act as scaffolds for the inclusion of *N*,*N*-dimethylaniline (DMA) molecules by donor−acceptor interactions. The resulting host−guest composite, DMA@**2**, shows desirably intense luminescence, which originated from photoinduced charge-transfer interactions in excited states.

Metal−organic frameworks (MOFs) with large pores and channels are being investigated for their diverse applications in gas storage, separation, catalysis, drug delivery, and sensing.[1] The combination of porosity with other properties allows the generation of multifunctional materials from MOFs. The host−guest chemistry of MOFs can be used to implement additional properties, such as guest-responsive switching, by loading the cavities with functional molecules, polymers, or even nanoparticles.[2] MOFs as solid host materials are being paid great attention when molecules, typically gases or small molecules, absorbed efficiently and their chemical and physical properties are subtly altered.[3] However, the study of photoinduced charge-transfer (CT) interactions between luminescent MOF hosts and confined guests in a nanosized space is relatively uncommon.[4]

CT interactions play a significant role in various functional materials. MOFs constructed with large π-conjugated molecules are useful as CT host materials. As is well-known, the trigonal-planar ligand with an electron-deficient triazine moiety, 4,4′,4″-*s*-triazine-2,4,6-triyltribenzoate (TATB), is an important organic building block for the construction of porous MOFs,[5−8] and additionally triazine rings typically arrange in a highly symmetric face-to-face $\pi-\pi$ stacking.[6] It can be predicted that a CT interaction would occur between a TATB-based MOF and an electron-rich guest molecule if electron-deficient triazine were directly incorporated into the pore walls of a MOF. The only example reported so far is a study on the guest-induced luminescent quenching of a ferrocene-loaded Tb^{III}TATB MOF through efficient CT.[7]

On the other hand, the stability of porous MOFs is key to including guest molecules. To improve the stability, one may apply secondary building block (SBU) stabilization, increased interaction between ligands in the form of $\pi-\pi$ stacking, or framework catenation.[5d,6] Interpenetration can stabilize the structure of a MOF against decomposition due to solvent loss or heating but can drastically reduce the size of the pores.[5d] Zhou's group reported a Zn^{II}-based porous MOF with a TATB ligand, $[Zn_3(TATB)_2(H_2O)_2\cdot solvent]_n$ (**1**),[6] which possesses interestingly a noninterpenetrated (10,3)-a net containing large chiral channels but is thermally unstable because of the easy removal of coordinated water molecules on the SBU. In this Communication, we give a desired strategy of increasing the thermal stability of compound **1** through an interpenetration route. Consequently, a novel doubly interpenetrated (10,3)-a net retaining large chiral channels, $[Zn_3(TATB)_2(H_2O)_2]_n$ (**2**), has been synthesized and characterized. Moreover, we also provide a strategy for the sake of achieving CT interaction between the host framework and guest molecules in excited states.

MOF **2** was successfully synthesized by varying the reaction temperature and reactant concentration [see the Supporting Information (SI)]. The phase purity of **2** was confirmed by powder X-ray diffraction (PXRD). Single-crystal X-ray diffraction analysis demonstrated that **2** crystallizes in tetragonal chiral space group $P4_22_12$; in contrast, **1** crystallizes in cubic chiral space group $P4_332$.[6] This different symmetry stems from the interpenetrated and noninterpenetrated lattices of **2** and **1**, respectively. Like **1**, the 3D structure of **2** is also composed of TATB Piedfort units and hourglass SBUs.[6] Each Piedfort unit connects three trimetallic hourglass SBUs. The whole structure of **2** displays a doubly interpenetrated framework with chiral (10,3)-a topology, as shown in Figure 1. Because of interpenetration, **2** has a second framework interwoven into the lattice, which results in a short linker−linker distance of 2.53 Å between two networks. This tightly interpenetrated structure may improve the thermal stability. In fact, thermogravimetric analysis (TGA) and variable-temperature PXRD indicated that the thermal stability of **2** is higher than that of **1**. The framework of **2** can be retained up to 350 °C (Figure 2a,e).

Although MOF **2** exhibits double interpenetration, the large square channels with triazine-based π walls are retained in the network viewed along the [001] and [110] directions (Figure 1a,b). However, the triangular channels along the [112] direction are dramatically decreased compared to **1** because of the interlocking interpenetration in this direction. The total solvent-accessible volume in the crystal structure of **2** is 4494.2 $Å^3$, and

Received: August 3, 2012
Published: February 1, 2013

   dx.doi.org/10.1021/ic301707h | *Inorg. Chem.* 2013, 52, 1667−1669

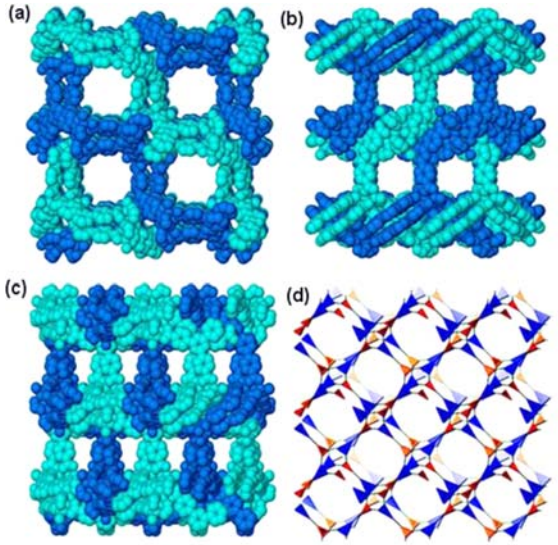

Figure 1. View of the doubly interpenetrated 3D framework with channels of **2** along the [001] (a), [110] (b), and [112] (c) directions and the chiral (10,3)-a network[5a] (d).

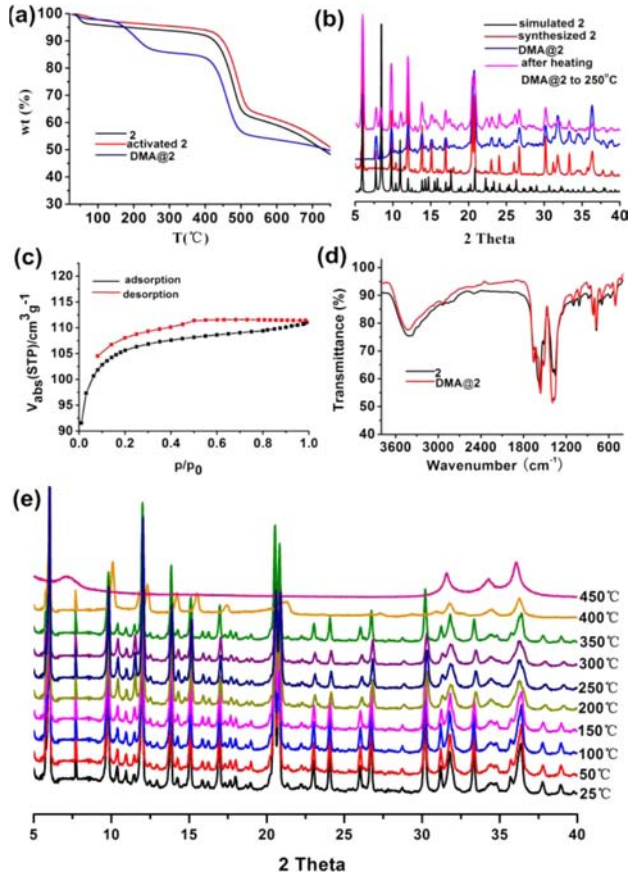

Figure 2. (a) TGA curves of **2**, activated **2**, and DMA@**2**. (b) XRPD patterns of simulated **2**, as-synthesized **2**, DMA@**2**, and DMA@**2** after heating to 250 °C. (c) Adsorption/desorption isotherm of N_2 for activated **2** at 77 K. (d) IR spectra of **2** and DMA@**2**. (e) Variable-temperature PXRD patterns of **2**.

the void volume is 53.8% of the total crystal volume (8351.4 Å^3), as calculated using the *PLATON* program.[8] To test the permanent porosity of **2**, gas adsorption studies were performed utilizing a fully activated sample. The N_2 sorption at 77 K for **2** was activated by evacuating a freshly prepared sample at 200 °C under a dynamic vacuum overnight. The stability of the activated sample was confirmed by TGA and PXRD. Fittings of the Brunauer–Emmett–Teller equation to the adsorption isotherms of N_2 (Figure 2c) give an estimated surface area of 355.68 m^2/g and a Langmuir surface area of 470.73m^2/g, which confirms the existence of micropores in **2**.

The stable and porous framework of **2** prompted examination of photoinduced CT interactions between the host electron-deficient triazine π walls and adsorbed electron-rich guests. *N*,*N*-Dimethylaniline (DMA) was selected as the guest molecule for its strong electron-donating ability.[4c] In order to avoid competition between adsorption of the solvent and adsorption of the desired guest molecules, we treated the crystals of **2** with CH_2Cl_2 for 5 days to exchange the attached dimethylformamide solvent, and then the resulting crystals were dried in a dynamic vacuum for 24 h to produce solvent-free materials (see the SI). DMA were fully adsorbed in the pores by immersion of dried **2** in liquid DMA, and excess DMA outside the host crystals was removed under reduced pressure. This resulted in the DMA-adsorbed form, DMA@**2**. The successful inclusion of DMA in **2** was evident because the colorless crystals turned green while maintaining their transparency (Figure 3a, inset). Moreover, it is

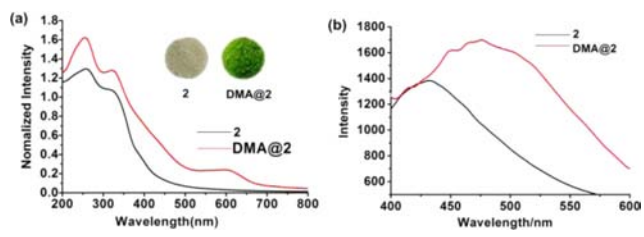

Figure 3. (a) Diffuse-reflectance UV–vis spectra of **2** and DMA@**2**. The inset shows photographic images of bulk samples **2** and DMA@**2**. (b) Emission spectra of **2** and DMA@**2** in the solid state at room temperature.

further confirmed by elemental analysis, IR, PXRD, and TGA measurements. DMA@**2** has a PXRD pattern and simulation similar to those of **2**; that is, the framework of **2** is stable when the guest molecules enter, except for some small peak shifts and new peaks, which indicates the presence of DMA guests (Figure 2b). The stepwise TGA curve and elemental analysis of DMA@**2** indicate that there are two DMA molecules entered per unit (Figure 2a). There is no further weight loss from 250 to 350 °C, which indicates that the host framework is stable after the loss of DMA guests, which is also confirmed by PXRD (Figure 2b).

The absorption spectra of **2** and DMA@**2** are shown in Figure 3a. The absorption maxima of **2** appear at 256 and 320 nm, which are attributed to the $\pi-\pi^*$ transitions of the TATB ligands. The absorption bands of DMA@**2** become broader, and a new band at around 600 nm appears, compared to those of **2**. The change indicates that the TATB units interact with the DMA guests in the ground state to form a CT complex in DMA@**2**. The solid-state emission spectra of **2** and DMA@**2** are depicted in Figure 3b. MOF **2** displays an emission maximum at 440 nm, which exhibits a significantly red-shifted emission compared to the noninterpenetrated MOF **1** (Em_{max} = 423 nm).[6] This effect can probably be attributed to the increased CT between linkers and Zn-based clusters (ligand-to-metal CT) that is possible in the more tightly interpenetrated structure.[9] Interestingly, the DMA@**2** emission spectrum is quite different from that of **2** and shows an intensive, broad, and red-shifted emission

dx.doi.org/10.1021/ic301707h | *Inorg. Chem.* 2013, 52, 1667–1669

maximum at 480 nm. The emission with a large Stokes shift represents an efficient photoinduced CT complex, an exciplex between the host triazine units (electron acceptor) and the guest DMA molecules (electron donor).[4c] Lifetimes of the emission for **2** and DMA@**2** are 1.15 and 1.53 ns, respectively. Upon inspection of the above results, the planarity of the TATB ligand and its tendency to encourage $\pi\cdots\pi$ stacking in MOF prove an extraordinary ability to increase the framework stability and a strong advantage in absorption and transformation of light energy, resulting in a preferential adjustment of the luminescence through CT.

In conclusion, a 3D doubly interpenetrated (10,3)-a network containing large channels has been synthesized, and the DMA guests successfully entered the host framework. The resulting host−guest composite shows intensive and tunable luminescence, which originated from photoinduced CT interactions in excited states. The observed features of **2** make it the candidate of desired materials in host−guest chemistry, and the inclusion of other guests in **2** is underway.

■ ASSOCIATED CONTENT

Ⓢ Supporting Information

X-ray crystallographic data in CIF format, experimental preparation, and crystal structure data. This material is available free of charge via the Internet at http://pubs.acs.org.

■ AUTHOR INFORMATION

Corresponding Author

*E-mail: hanlei@nbu.edu.cn. Tel: +86 574 87600782.

Notes

The authors declare no competing financial interest.

■ ACKNOWLEDGMENTS

This work was supported by the National Natural Science Foundation of China (Grants 21071087 and 91122012), the Scientific Research Foundation for the Returned Overseas Chinese Scholars, the Outstanding Dissertation Growth Fundation of Ningbo University, and the K. C. Wong MagnaFund in Ningbo University.

■ REFERENCES

(1) (a) O′Keeffe, M.; Yaghi, O. M. *Chem. Rev.* **2012**, *112*, 675−702. (b) Sumida, K.; Rogow, D. L.; Mason, J. A.; McDonald, T. M.; Bloch, E. D.; Herm, Z. R.; Bae, T.-H.; Long, J. R. *Chem. Rev.* **2012**, *112*, 724−781. (c) Li, J.-R.; Sculley, J.; Zhou, H.-C. *Chem. Rev.* **2012**, *112*, 869−932. (d) Kreno, L. E.; Leong, K.; Farha, O. K.; Allendorf, M.; Van Duyne, R. P.; Hupp, J. T. *Chem. Rev.* **2012**, *112*, 1105−1125. (e) Yoon, M.; Srirambalaji, R.; Kim, K. *Chem. Rev.* **2012**, *112*, 1196−1231. (f) Horcajada, P.; Gref, R.; Baati, T.; Allan, P. K.; Maurin, G.; Couvreur, P.; Férey, G.; Morris, R. E.; Serre, C. *Chem. Rev.* **2012**, *112*, 1232−1268.

(2) (a) Chae, H. K.; Siberio-Pérez, D. Y.; Kim, J.; Go, Y.; Eddaoudi, M.; Matzger, A. J.; O′Keeffe, M.; Yaghi, O. M. *Nature* **2004**, *427*, 523−527. (b) Inokuma, Y.; Kawano, M.; Fujita, M. *Nat. Chem.* **2011**, *3*, 349−358. (c) Juan-Alcañiz, J.; Gascon, J.; Kapteijn, F. *J. Mater. Chem.* **2012**, *22*, 10102−10118. (d) Müller, M.; Devaux, A.; Yang, C.-H.; Cola, L. D.; Fischer, R. A. *Photochem. Photobiol. Sci.* **2010**, *9*, 846−853. (e) Hermes, S.; Schröter, M.-K.; Schmid, R.; Khodeir, L.; Muhler Tissler, A.; Fischer, R. W.; Fischer, R. A. *Angew. Chem., Int. Ed.* **2005**, *44*, 6237−6341. (f) Uemura, T.; Yanai, N.; Kitagawa, S. *Chem. Soc. Rev.* **2009**, *38*, 1228−1236.

(3) (a) Stylianou, K. C.; Heck, R.; Chong, S. Y.; Bacsa, J.; Jones, J. T. A.; Khimyak, Y. Z.; Bradshaw, D.; Rosseinsky, M. J. *J. Am. Chem. Soc.* **2010**, *132*, 4119−4130. (b) Yanai, N.; Uemura, T.; Inoue, M.; Matsuda, R.; Fukushima, T.; Tsujimoto, M.; Isoda, S.; Kitagawa, S. *J. Am. Chem. Soc.* **2012**, *134*, 4501−4504. (c) Potts, S. V.; Barbour, L. J.; Haynes, D. A.; Rawson, J. M.; Lloyd, G. O. *J. Am. Chem. Soc.* **2011**, *133*, 12948−12951. (d) Haneda, T.; Kawano, M.; Kojima, T.; Fujita, M. *Angew. Chem., Int. Ed.* **2007**, *46*, 6643−6645.

(4) (a) Ohmori, O.; Kawano, M.; Fujita, M. *J. Am. Chem. Soc.* **2004**, *126*, 16292−16293. (b) Shimomura, S.; Matsuda, R.; Tsujino, T.; Kawamura, T.; Kitagawa, S. *J. Am. Chem. Soc.* **2006**, *128*, 16416−16417. (c) Tanaka, D.; Horike, S.; Kitagawa, S.; Ohba, M.; Hasegawa, M.; Ozawa, Y.; Toriumi, K. *Chem. Commun.* **2007**, 3142−3144. (d) Yao, Q.-X.; Pan, L.; Jin, X.-H.; Li, J.; Ju, Z.-F.; Zhang, J. *Chem.—Eur. J* **2009**, *15*, 11890−11897. (e) Ohara, K.; Inokuma, Y.; Fujita, M. *Angew. Chem., Int. Ed.* **2010**, *49*, 5507−5509. (f) Shimomura, S.; Kitagawa, S. *J. Mater. Chem.* **2011**, *21*, 5537−5546.

(5) (a) Zhao, D.; Timmons, D. J.; Yuan, D.-Q.; Zhou, H.-C. *Acc. Chem. Res.* **2011**, *44*, 123−133. and references cited therein. (b) Gao, W.; Xing, F.-F.; Zhou, D.; Shao, M.; Zhu, S.-R. *Inorg. Chem. Commun.* **2011**, *14*, 601−605. (c) Zhang, H.-B.; Li, N.; Tian, C.-B.; Liu, T.-F.; Du, F.-L.; Lin, P.; Li, Z.-H.; Du, S.-W. *Cryst. Growth Des.* **2012**, *12*, 670−678. (d) Ma, S.-Q.; Wang, X.-S.; Yuan, D.-Q.; Zhou, H.-C. *Angew. Chem., Int. Ed.* **2008**, *47*, 4130−4133.

(6) Sun, D.-F.; Ke, Y.-X.; Collins, D. J.; Lorigan, G. A.; Zhou, H.-C. *Inorg. Chem.* **2007**, *46*, 2725−2734.

(7) Park, Y. K.; Choi, S. B.; Kim, H.; Kim, K.; Won, B.-H.; Choi, K.; Choi, J.-S.; Ahn, W.-S.; Won, N.; Kim, S.; Jung, D. H.; Choi, S.-H.; Kim, G.-H.; Cha, S.-S.; Jhon, Y. H.; Yang, J. K.; Kim, J. *Angew. Chem., Int. Ed.* **2007**, *46*, 8230−8233.

(8) Spek, A. L. *J. Appl. Crystallogr.* **2003**, *36*, 7−13.

(9) Meek, S. T.; Houk, R. J. T.; Doty, F. P.; Allendorf, M. D. *ECS Trans.* **2010**, *28*, 137−143.